



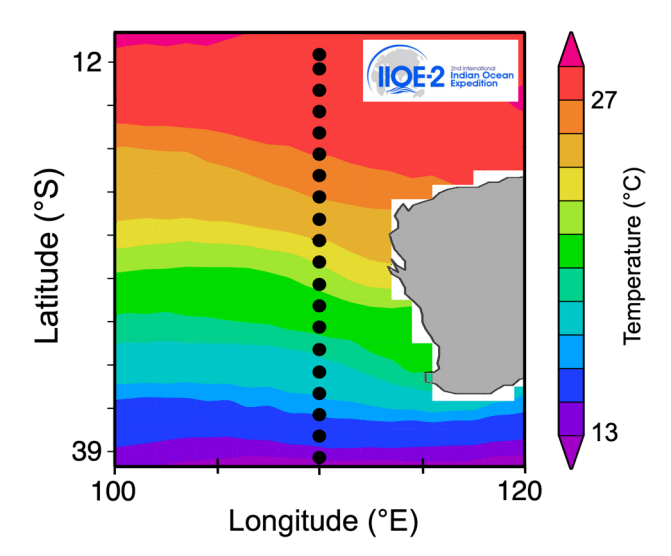


Mesozooplankton biomass and temperature-enhanced grazing along a 110°E transect in the eastern Indian Ocean

Michael R. Landry^{1,*}, Raleigh R. Hood², Claire H. Davies³

¹Scripps Institution of Oceanography, University of California at San Diego, La Jolla, CA 92093-0227, USA ²Horn Point Laboratory, University of Maryland Center for Environmental Science, Cambridge, MD 21613, USA ³CSIRO Oceans and Atmosphere Flagship, Castray Esplanade, Hobart, Tasmania 7000, Australia

ABSTRACT: Low-latitude waters of the Indian Ocean are warming faster than other major oceans. Most models predict a zooplankton decline due to lower productivity, enhanced metabolism and phytoplankton size shifts that reduce trophic transfer efficiency. In May-June 2019, we investigated mesozooplankton biomass and grazing along the historic 110°E transect line from the International Indian Ocean Expedition (IIOE) of the 1960s. Twenty sampling stations from 39.5 to 11.5° S spanned latitudinal variability from temperate to tropical waters and a pronounced 14°C gradient in mean euphotic zone temperature. Although mesozooplankton size structure was similar along the transect, with smaller (<2 mm) size classes dominant, total biomass increased 3-fold (400 to 1500 mg dry weight m⁻²) from high to low latitude. More dramatically, gut-fluorescence estimates of grazing (total ingestion or % euphotic zone chl a consumed d^{-1}) were 14- and 20-fold higher, respectively, in the low-latitude warmer waters. Biomass-normalized grazing rates varied more than 6-fold over the transect, showing a strong temperature relationship $(r^2 = 0.85)$ that exceeded the temperature effects on gut turnover and metabolic rates. Herbivory contributed more to satisfying zooplankton energetic requirements in low-chl a tropical waters than chl a-rich waters at higher latitude. Our unexpected results are inconsistent with trophic amplification of warming effects on phytoplankton to zooplankton, but might be explained by enhanced coupling efficiency via mixotrophy. Additional implications for selective herbivory and topdown grazing control underscore the need for rigorous field studies to understand relationships and validate assumptions about climate change effects on the food webs of tropical oceans.



Sea surface temperature gradient ($2^{\circ} \times 2^{\circ}$ smoothed) and 110° E transect stations (dots) off of western Australia in May 2019.

Graphic: NOAA Physical Sciences Laboratory, adapted by M. Landry

KEY WORDS: Zooplankton \cdot Biomass \cdot Grazing \cdot Gut fluorescence \cdot Growth \cdot Respiration \cdot Carbon demand \cdot Mixotrophy \cdot Trophic amplification

1. INTRODUCTION

Despite its many unique features and climate system importance, the Indian Ocean has long been an understudied ocean. This led to a major international effort in the 1960s, the International Indian Ocean Expedition (IIOE), to establish basic knowledge of

© The authors 2020. Open Access under Creative Commons by Attribution Licence. Use, distribution and reproduction are unrestricted. Authors and original publication must be credited.

Publisher: Inter-Research · www.int-res.com

the region and, more recently, to the initiation of a second international effort (IIOE-2) for advanced studies of the region's dynamics relevant to climate, biogeochemical cycles, ecosystems and fisheries. The current study was conducted as part of IIOE-2 on a cruise that retraced the historic 110°E transect sampled bi-monthly by Australian oceanographers from 1962–1963. That study was the first integrated investigation of circulation, nutrients, primary productivity and zooplankton in the eastern Indian Ocean and led in its time to many new insights about distributional relationships and seasonality in the region (Humphrey & Kerr 1969, Jitts 1969, Newell 1969, Rochford 1969, 1977, Tranter 1977a,b, Tranter & Kerr 1969, 1977).

Our study reports paired day and nighttime measurements of mesozooplankton biomass and grazing at 20 stations from 39.5 to 11.5°S that comprise most of the latitudinal variability off western Australia from temperate/subantarctic to tropical waters. The original IIOE investigations showed a south-to-north biomass increase along this transect (Tranter & Kerr 1969, 1977). We expected a similar trend, consistent with the general low-latitude (tropical) enrichment of biomass in the global zooplankton database (Moriarty & O'Brien 2013, Moriarty et al. 2013). Nonetheless, we considered the possibility that IIOE measurements might have misrepresented temporal or spatial patterns in having only been made as wet weight, analogous to documented issues with displacement volume measurements. In the California Current, for example, Roemmich & McGowan (1995) reported an 80% decline in zooplankton (volume) biomass associated with the switch from cold to warm phase of the Pacific Decadal Oscillation. A more careful analysis, however, revealed that this decrease was mainly due to differences in the abundance of salps, which disproportionally impacted the volume measurements, with little effect on major taxa or carbon (C) biomass (Lavaniegos & Ohman 2003). To avoid such issues with gelatinous taxa and to assess latitudinal variability in zooplankton size structure, we size-fractionated our zooplankton samples and determined dry weight (DW), C and nitrogen (N) values for each fraction.

Grazing rates were not measured on the original IIOE voyages nor, to the best of our knowledge, in any study assessing latitudinal variability in the eastern Indian Ocean over the past 5 decades. Nonetheless, based on the general view that most phytoplankton in warm, low-nutrient systems would be too small to be grazed directly by mesozooplankton, we expected that variability in measured rates would

largely follow differences in trophic richness, for which increasing chlorophyll a (chl a) would be an indicator of more total phytoplankton and greater relative biomass of larger forms (e.g. Taylor & Landry 2018). What we found instead were relatively consistent conditions of low nutrients and low chl a throughout the subtropical and tropical water masses but a very pronounced gradient in temperature, which emerged as the master variable of the study. Biomass-specific grazing estimates were shown to be strongly related to temperature, increasing dramatically along the transect and exceeding the effect of higher temperature on zooplankton C demand for respiration and growth. This unexpected finding suggests a more efficient trophic linkage between phytoplankton and zooplankton in warm tropical waters than generally assumed and does not fit the view of the negative impacts of ocean warming on phytoplankton being amplified for zooplankton (Chust et al. 2014, Stock et al. 2014, Kwiatkowski et al. 2019).

2. MATERIALS AND METHODS

2.1. Zooplankton sample collection

Zooplankton samples were collected at 20 stations on the 110°E transect from 17 May to 5 June 2019 on R/V 'Investigator' cruise IN2019v03 (Fig. 1). The stations, spaced 1.5° apart from 39.5 to 11.5°S, were sampled on successive days according to a fixed time schedule. At each station, we took 2 samples with a 1 m diameter ring net towed obliquely through the euphotic zone at a ship speed of 1.5 knots. The first net tow was conducted at mid-day (13:32 h \pm 16 min, SD); the second tow was taken during the dark (19:32 \pm 8 min), 1–2 h after local sunset. We refer to these below as 'day' and 'night' tows, the difference between them representing the nocturnal entry of diel vertical migrants into the euphotic zone. The plankton net was made with 0.2 mm mesh Nitex and equipped with a General Oceanics flowmeter attached across the mouth and a Senus Ultra timedepth-temperature recorder (ReefNet) fastened to the frame. Mean (±SD) tow depth and volume sampled, assuming 100% net efficiency, were 104 ± 19 m and 342 ± 67 m³, respectively. Nominal depths of the euphotic zone, estimated as the depth of 1% surface irradiance from photosynthetically active radiation (PAR) extinction coefficients on CTD casts preceding the daytime net tow at each station, ranged from 66 to 108 m and averaged 86 ± 12 m for the transect.

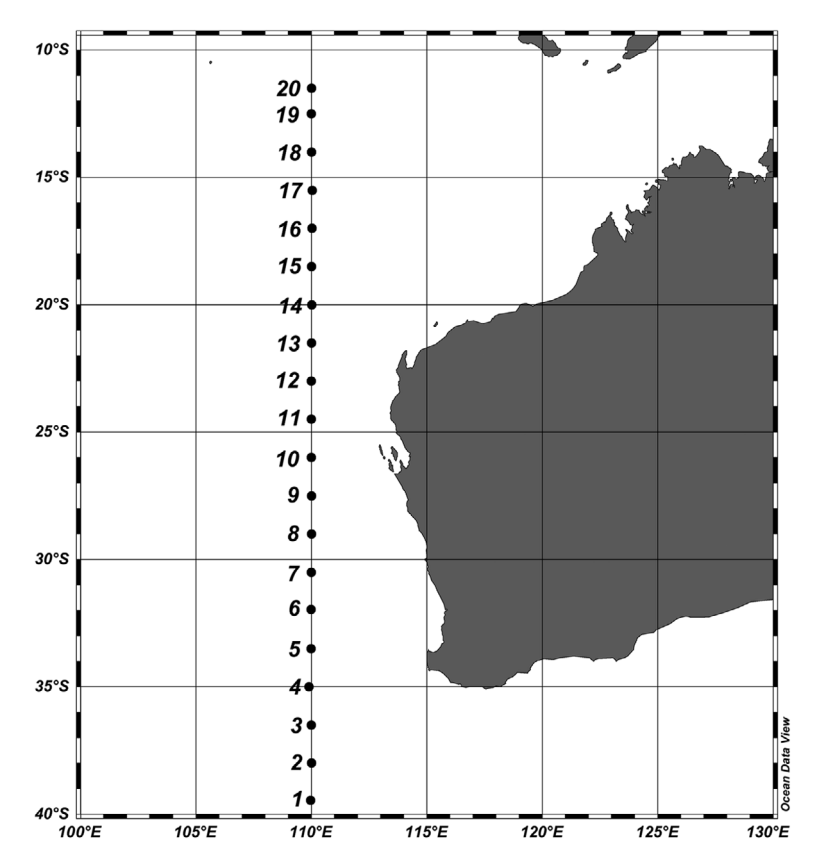


Fig. 1. Station locations along 110°E sampling transect in the eastern Indian Ocean off Western Australia

Upon retrieval, the contents of the net codend were anesthetized with CO_2 (ice-cold soda water; Kleppel & Pieper 1984) and the entire cod end was placed in a bucket with a freshly made ice slurry (–1.8°C) from an on-board seawater ice maker to slow metabolism and gut evacuation of the zooplankton. Codend contents were subsampled with a Folsom plankton splitter. Generally, half of the tow was preserved in borate-buffered 10% formalin. The remaining half was split again to obtain $^{1}\!\!/4$ subsamples for biomass and gut pigment analyses. Because gut pigment samples are more time-sensitive, they were processed first.

Gut pigment subsamples were sorted by wet sieving through nested Nitex screens of 5, 2, 1, 0.5 and 0.2 mm Nitex mesh to produce 5 size classes of 0.2–0.5, 0.5–1, 1–2, 2–5 and >5 mm. The nested screen stack was partially submerged in a shallow basin filled with ice-cold seawater, and the sample was poured into the upper (5 mm) screen and worked through successive screen layers using a squirt bottle filled with 0.2 μ m filtered water. The organisms retained on each mesh were concentrated onto a separate 47 mm glass-fiber filter, placed in a small cov-

ered petri dish, and frozen at -20°C for one to several hours before shipboard processing.

The net tow subsamples for biomass analyses were similarly size-fractioned through the nested filters and concentrated onto preweighed filters (47 mm diameter) made from 0.2 mm Nitex. These samples were rinsed with isotonic ammonium formate solution to remove interstitial sea salt, placed in individual petri dishes and oven-dried on shipboard at 50°C for several days to a week. Covered petri dishes containing the dried samples were packed in an airtight container with silica gel packets and taken back to the laboratory for analysis.

2.2. Measurements of DW, C and N biomass

In the laboratory, dried net tow samples from the cruise were oven-dried additionally at 60°C for 24 h before weighing. For each size-fractioned sample, zooplankton DW (mg m⁻²) was calculated from the difference between initial and final weights of the filter, the measured volume and depth of the tow, and the fraction of sample analyzed. The dried sample was subsequently scraped off

the filter, ground to a powder with a mortar and pestle and subsampled by weight for C and N analyses.

The CN subsamples were weighed in small tin boats, packed into pellets, and analyzed with a Perkin Elmer CHN analyzer. Acetanilide was used as the standard for instrument stability on every run. C and N biomass estimates (mg m⁻²) for euphotic zone zooplankton were computed for each size fraction from C:DW and N:DW ratios and measured DWs.

2.3. Gut pigment and grazing estimates

Gut pigment samples were analyzed on shipboard within 24 h of collection. For all <5 mm size fractions, the frozen filters were sectioned into quarters with a razor blade, and duplicate representative quarters were prepared for analysis. The remaining $\frac{1}{2}$ samples were kept frozen in the petri dishes as backup for possible processing issues but were eventually discarded at the end of the cruise. For most of the >5 mm fractions, the organisms were too few and non-randomly dispersed for quantitative sectioning. These samples were analyzed whole, typically by cutting out and

combining the portions of the filter with organisms on them. All samples were placed in 15 ml polypropylene test tubes (BD Falcon) with 7 ml of 90% acetone and homogenized (multiple 20 s bursts) in an ice bath with a Vibracell sonicator probe. They were then extracted overnight (18-24 h) in a -20°C freezer and warmed to room temperature in a dark container prior to analysis. The homogenate was shaken and centrifuged (5 min at 3000 rpm, $1000 \times g$) to remove particulates. Concentrations of chl a and phaeopigments (Phaeo) were then measured by the acidification method using a 10AU fluorometer (Strickland & Parsons 1972). Water-column estimates of depth-integrated chl a for the euphotic zone were made similarly from analyses of 0.5 l samples collected from the evening CTD hydrocast, extracted for 24 h in 90 % acetone and measured on the same fluorometer.

For each size-fraction analyzed, we computed the depth-integrated concentration of gut pigment (chl a, Phaeo) in the euphotic zone as:

$$GPC = \frac{pig \times D}{vol \times f} \tag{1}$$

where GPC is gut pigment content (mg m⁻²), pig is the measured pigment value (mg), f is fraction of sample analyzed, D is depth of tow (m) and vol is the volume of water filtered (m³). To be conservative, we based our zooplankton grazing estimates on measured gut Phaeo values only, without correction for inefficiencies in converting chl a into Phaeo. Conover et al. (1986) showed, for example, that the common practice of multiplying Phaeo estimates by a factor of 1.51 (the chl a: Phaeo weight ratio) was redundant with standard fluorometric equations that already compute Phaeo values in terms of chlorophyll weight equivalents. Durbin & Campbell (2007) further argued that Phaeo degradation to non-fluorescent products during digestion is accounted for in experimental determinations of gut evacuation rate.

We estimated grazing rates (G, mg pigment m⁻² time⁻¹) for each size fraction and for the total zooplankton assemblage as $G = GPC \times K$, where $K(\min^{-1})$ is the gut evacuation rate constant. For K, we used the mean temperature-dependent relationship, $K = 0.0026(T^{\circ}C) + 0.012$, from the literature review of Irigoien (1998). Landry et al. (1994) previously noted that the exponential temperature function $K = 0.0121e^{0.0864T}$ from Dam & Peterson (1988) gave values close to field-measured rate constants at 17.5–19°C, and so that relationship was also considered. Fig. 2 illustrates the difference between these 2 functions for the range of mean euphotic zone temperatures in our study. While neither function is well constrained by data at the higher environmental temperatures that we encoun-

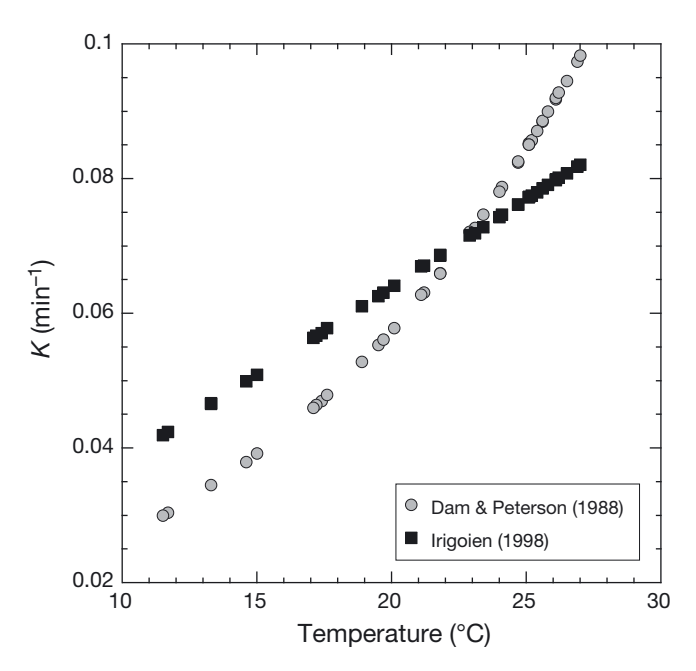


Fig. 2. Comparison of gut clearance rate constants (K) for mesozooplankton, calculated with temperature functions of Dam & Peterson (1988) and Irigoien (1998) for mean euphotic zone temperatures on the 110°E transect recorded in day and night net tows

tered, the linear extrapolation of Irigoien (1998) was deemed more appropriate because it represented a more conservative (2-fold vs. 3-fold) rate constant range for our grazing calculations and because it was based on more data, including those of Dam & Peterson (1988) and Landry et al. (1994).

To compute biomass-specific rates of phytoplankton grazing by the zooplankton assemblage and individual size classes, we calculated $G \times B^{-1}$, where B is biomass expressed as mg DW m $^{-2}$ or mg C m $^{-2}$. Daily removal rates of phytoplankton by zooplankton grazing were computed as $G \times chl_z^{-1}$, where chl_z is the depthintegrated concentration of chl a in the euphotic zone (mg chl a m $^{-2}$). Lastly, day–night differences in grazing rates were computed from the paired day/night net tows at each station. All statistical tests (Pearson correlation, t-test) were done in Excel Data Analysis with significance defined by $\alpha = 0.05$, 2-tailed.

3. RESULTS

3.1. Study site characteristics during May–June 2019

The main feature of temperature variability along the 110°E transect was a relatively uniform, monotonic increase from 12°C in the south to 28°C in the north (Fig. 3, Table 1). This temperature gradient applied not only to the mixed layer but also extended more broadly to the depth of the euphotic zone (1% incident PAR penetration), as indicted by the mean temperature over the upper 100 m (Table 1). Despite the lack of prominent temperature discontinuities in the upper waters, temperature–salinity (T-S) charac-

teristics defined 2 major water masses as well as frontal and mixing zones along the transect. The high-salinity surface water (>35.7 psu) between ~27.5° and 35°S (Stns 4–9) is South Indian Central Water (SICW), a distinctive feature of the southern Indian Ocean subtropical region that sinks below lower density water to the north (Rochford 1969, Woo

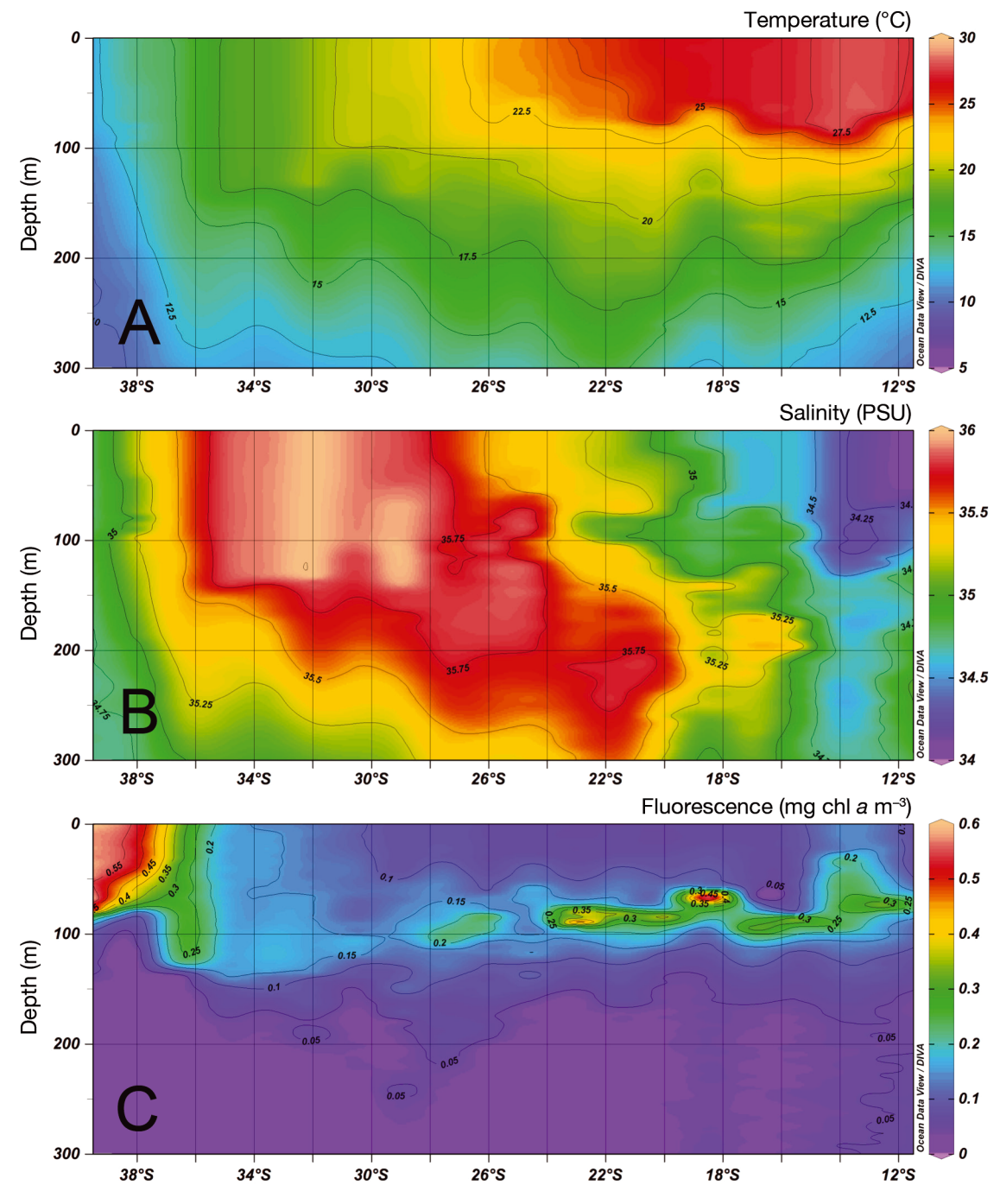


Fig. 3. Upper ocean (0–300 m) sections of environmental variability along the 110°E transect. (A) Temperature; (B) salinity; (C) chlorophyll *a* fluorescence. All data are continuous profiles from CTD hydrocasts

Table 1. Environmental data for the 110°E sampling stations. MLD: surface mixed-layer depth, defined as the depth at which temperature decreases 0.1°C below surface values. DCM: depth of maximum chl a fluorescence in CTD profiles. 1% I_0 : the nominal depth of the euphotic zone defined by light (photosynthetically active radiation) extinction. $T_{\rm ML}$, $S_{\rm ML}$, chl_{ML}: mean values for temperature, salinity and extracted chlorophyll of the surface mixed layer. $T_{\rm mean}$: mean integrated temperature of the upper 100 m. Nitr_{100m} and chl_{100m}: depth-integrated values of NO₃⁻ and chl a to 100 m

Stn	Lat. (°S)	MLD (m)	DCM (m)	1 % I _o (m)	$T_{ m ML}$ (°C)	$S_{ m ML}$ (psu)	Chl _{ML} (mg m ⁻³)	$T_{ m mean}$ (°C)	$\mathrm{Nitr_{100m}}\ (\mathrm{mmol}\ \mathrm{m}^{-2})$	Chl _{100m} (mg m ⁻²)
1	39.5	74	31	71	12.2	34.80	0.26	12.1	772	37.5
2	38.0	39	19	66	13.9	33.65	0.58	13.5	466	29.9
3	36.5	119	11	74	15.3	35.53	0.21	15.2	51.8	24.2
4	35.0	79	61	102	18.0	35.85	0.27	17.8	3.5	20.2
5	33.5	129	71	86	18.2	35.91	0.31	18.1	2.4	26.7
6	32.0	141	61	105	19.5	35.99	0.20	19.4	2.4	20.3
7	30.5	91	108	92	20.3	35.90	0.32	20.3	2.4	32.9
8	29.0	48	76	108	20.8	35.84	0.10	20.5	3.5	19.9
9	27.5	18	91	90	21.7	35.70	0.29	21.4	8.7	43.0
10	26.0	34	85	91	23.7	35.46	0.10	23.0	4.5	17.7
11	24.5	35	78	83	24.2	35.39	0.13	23.2	16.9	24.5
12	23.0	37	78	84	25.0	35.27	0.15	24.0	40.7	28.2
13	21.5	33	86	100	25.7	35.17	0.08	24.7	56.0	20.9
14	20.0	20	82	85	26.6	34.92	0.11	25.6	81.4	27.5
15	18.5	50	57	68	26.8	34.75	0.15	24.9	301	12.1
16	17.0	60	87	87	27.0	34.59	0.13	26.3	12.3	15.5
17	15.5	75	90	85	27.3	34.60	0.16	26.6	27.4	22.9
18	14.0	77	83	81	28.1	34.28	0.42	27.7	81.5	31.5
19	12.5	64	74	91	27.9	34.16	0.10	26.5	186	22.2
20	11.5	58	66	80	28.1	34.18	0.07	26.5	308	23.5

& Pattiaratchi 2008). We refer to this generically as subtropical surface water (Wyrtki 1973). The hightemperature, low-salinity water mass north of 14°S (Stns 18-20) is water that enters the Indian Ocean from the Pacific via the Indonesian Throughflow (ITF) and is variously referred to as Australasian Mediterranean Water (Tomczak & Godfrey 1994, Wijffels et al. 2002), ITF water or Tropical Surface Water (Woo & Pattiaratchi 2008). Between the subtropical and tropical/ITF surface waters is a broad zone (15.5-26°S, Stns 10-17) of high eddy activity and mixing with intermediate T-S properties and a subsurface salinity maximum between 150 and 250 m. South of the SICW (>36°S, Stns 1-3) is the Subtropical Front, where colder, lower salinity subantarctic water converges with and subducts under the subtropical water mass.

Chlorophyll profiles from the CTD fluorometer showed the highest values on the southern (subantarctic) side of the Subtropical Front, with a sharp boundary between high and low mixed-layer values at $\sim 36^{\circ}$ S (Fig. 3, Table 1). While a subsurface chl a maximum could be found in all traces, it was rather weakly defined in profiles south of 28° S and only became a prominent feature of the chl a distributions north of 24° S. Consistent with chl a variability, depth-integrated (0–100 m) nitrate inventories were

highest on the subantarctic side of the Subtropical Front and lowest in the subtropical region immediately to the north (Table 1). Depth-integrated nitrate concentrations (Nitr $_{100m}$) also rose through the tropical and mixing regions north of 25° S. This mainly reflects a trend toward shallower euphotic depths in this area (i.e. a larger portion of the nitracline is sampled in the upper 100 m), as mixed-layer nutrient concentrations generally remain very low throughout the subtropical and topical regions.

3.2. Mesozooplankton biomass variability along 110° E

Mesozooplankton DWs for the 110°E transect varied from a low value of 320 mg m⁻² for the day tow at 38°S to 1930 mg m⁻² for the night tow at 14°S (Fig. 4). On average, biomass of night collections exceeded day tows by 50%, indicating that migratory zooplankton typically account for one-third of the nighttime biomass. However, this ratio was notably variable along the transect, especially at the southern end. For instance, 2 of the 4 most southern stations had slightly higher biomass during the day tow than at night, suggesting that diel vertical migration is less expressed in that region, at least during our sampling

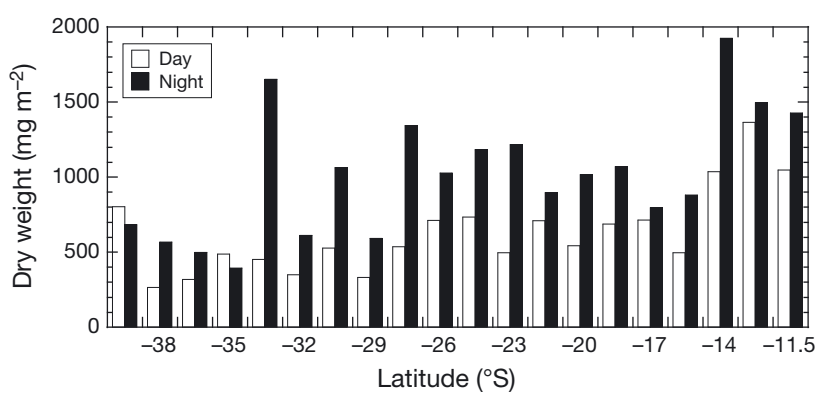


Fig. 4. Daytime and nighttime estimates of mesozooplankton dry weights for tows along the 110°E transect in May–June 2019

period. In contrast, at neighboring Stn 5 (33.5°S), the night:day biomass ratio (3.7) exceeded that at any other sampling location. The nighttime biomass at this station was dominated by large euphausiids in the 2–5 mm size fraction. In addition, a mesopelagic fish (Myctophum phengodes; 8.7 cm length, 8.8 g wet weight), the largest specimen collected in all of the transect tows, was excluded from the night biomass estimate at Stn 5, but would have elevated the night:day biomass ratio to 5.0 if included. The unusually high night:day biomass ratio at 33.5°S might be

explained by its proximity to the Subtropical Front, where water and organisms from the richer southern habitat are transported and concentrated beneath poorer SICW to the north.

Mean mesozooplankton biomass from combined day and night tows increased from south to north, with the highest values of 1380 ± 126 mg DW m⁻² in the tropical/ITF water, the lowest values of $498 \pm 165 \text{ mg DW m}^{-2}$ in subantarctic water around the Subtropical Front and intermediate values (794 \pm 171 mg DW m⁻²) in the subtropical and mixing regions (Fig. 5A). In contrast to the variability in total biomass, size class contributions were reasonably consistent across the transect, except that smaller zooplankton accounted for a slightly larger proportion of biomass in the richer, colder habitat of the subantarctic region (Fig. 5B). Overall, 0.2-0.5, 0.5-1, 1-2 and 2-5 mm size fractions comprised 21 ± 5 , 24 ± 5 , 27 ± 4 and $22 \pm 7\%$, respectively, of total zooplankton DW for the transect.

To calculate mesozooplankton C biomass from DW measurements, we applied C:DW conversion factors determined for each size class and sampling station. Conversion factors for night tows were ~1% higher on average than for day tows, but the 2 tows were combined for station size-class means (Fig. 6). All size fractions displayed a maximum–minimum difference in C content of at least 10% and up to 15% of DW over the transect. The 3 smaller size classes, dominated by crustaceans (copepods, euphausiids), had similar mean values (35.6 ± 3.2 to $34.5 \pm 4.1\%$

for the 0.2–0.5 and 1–2 mm fractions, respectively). They also exhibited similar latitudinal patterns, with local minima (24–30%) in subtropical waters from 32–35° S (Stns 4–6) and maximum values (~40%) in transition waters from 18.5–20° S (Stns 14–15). The 2–5 mm fraction, comprising a greater proportion of gelatinous taxa, stood out as being distinctly different from the smaller size classes, with a substantially lower mean C content (27.7 \pm 4.0%) and an abrupt shift between consistently low values (~24%) south of 28° S and higher values to the north (~30%, except

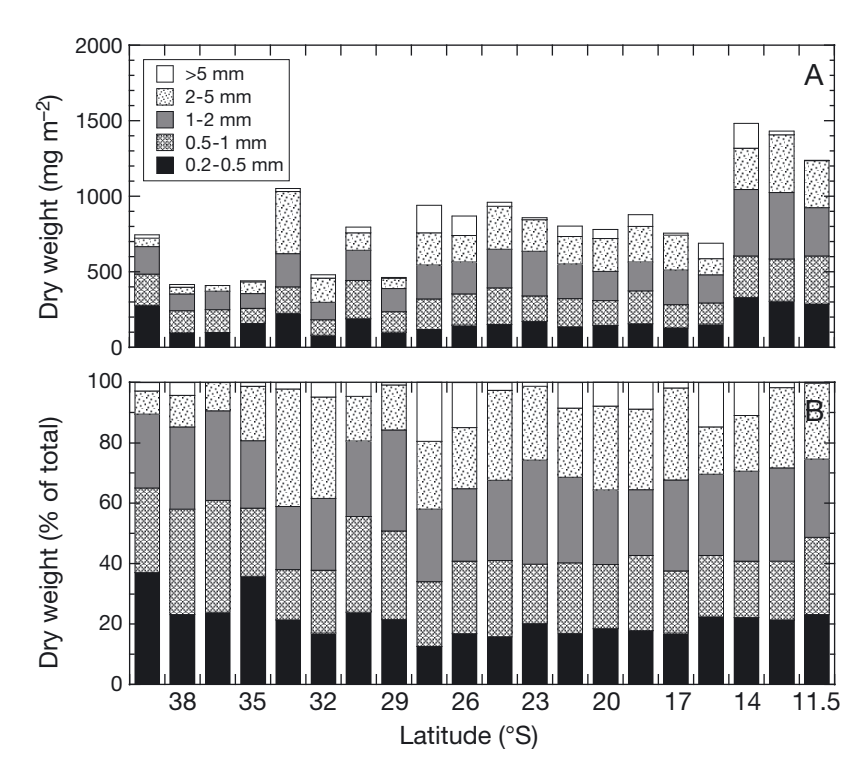


Fig. 5. Mesozooplankton size structure along the 110°E transect. (A) Mean size-fractioned dry weights from combined day and night tows; (B) % contributions of size fractions to total dry weight

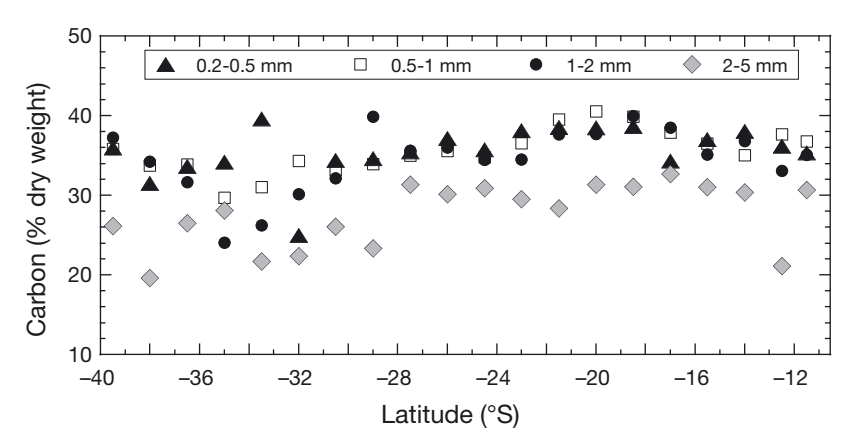


Fig. 6. Latitudinal and size class variability in mesozooplankton carbon content as percent of dry weight. Each data point is the mean of analyses for day and night tows

for Stn 19). C:DW values were lowest on average $(20.1 \pm 7.6\%)$ for >5 mm zooplankton, but those data were not plotted in Fig. 6 because they were sparse and highly variable, comprising only a few specimens from diverse taxa in each tow. Because the C:DW ratio decreased on average with increasing zooplankton size (Fig. 6), the relative importance of smaller size fractions (0.2-2 mm) is greater (78%) in terms of C biomass compared to DW

(72%; Fig. 5).

While we did not use C:N conversions in the present study, our transect-averaged ratios varied narrowly from 4.14-4.26 for all <5 mm zooplankton size classes. An overall mean value of 4.21 ± 0.36 (n = 160) would therefore be broadly applicable to the community as a whole. The complete data set for size-fractioned DW, C and N values is provided in Table S1 in the Supplement at www.int-res.com/articles/suppl/m649p001_supp.pdf.

3.3. Grazing rate estimates

While mean biomass varied only about 3-fold over the transect (Fig. 5), grazing rate estimates showed more substantial increases from higher to lower latitudes (Fig. 7). Estimates of phytoplankton consumption ranged 14-fold from the lowest values of ~ 0.3 mg chl a m $^{-2}$ d $^{-1}$ south of 32° S (Stns 1, 3 and 6) to the highest values of ~ 3.6 mg chl a m $^{-2}$ d $^{-1}$ in the tropical

region north of 14° S (Stns 18 and 20) (Fig. 7A). Grazing impact by zooplankton, calculated as the percentage of euphotic-zone chl a consumed d^{-1} , showed an even greater 20-fold range from 1.2% at 39.5° S (Stn 1) to 24.3% at 11.5° S (Stn 20), with a relatively smooth increasing trend at intermediate latitudes (Fig. 7B).

Chl *a* ingestion estimates rose gradually through the subtropical and subtropical–tropical mixing regions despite little difference in depthintegrated chl *a*, and a slight (but not statistically significant; $r_{18} = 0.31$, p = 0.18) decreasing trend in chl_{100m} over this area (Fig. 7A, Table 1). Similar

to biomass measurements, smaller (<2 mm) size fractions dominated grazing all along the transect. On a relative basis, however, larger zooplankton contributed more to grazing in the warmer waters north of 20° – 21.5° S compared to cooler and richer waters to the south (Fig. 7A), reflecting our observations of more occasional small salps in the tropical waters.

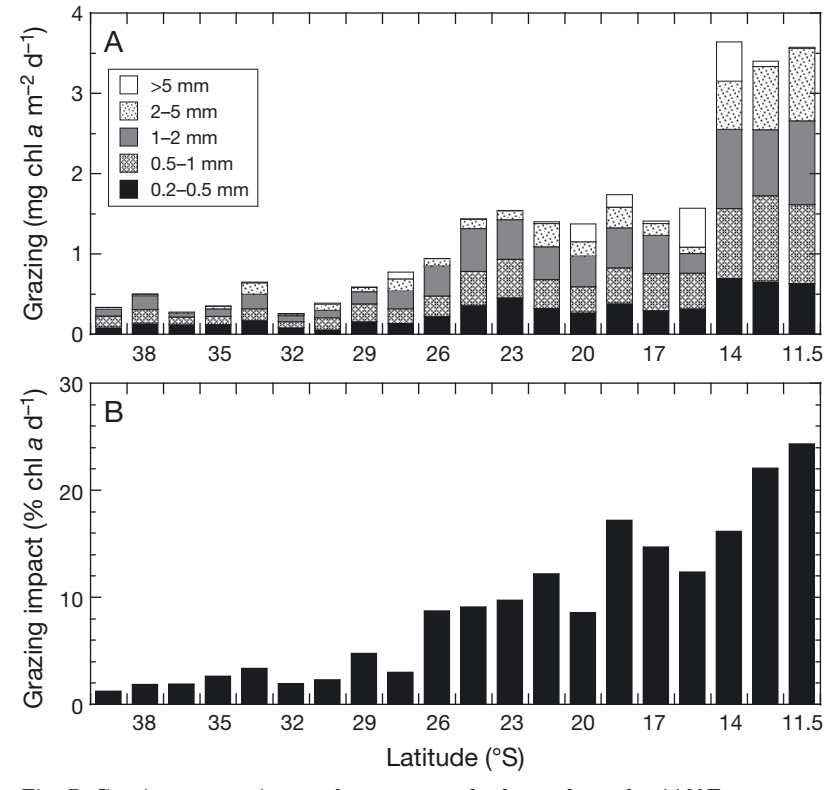


Fig. 7. Grazing rate estimates for mesozooplankton along the 110°E transect. (A) Contributions of zooplankton size fractions to total daily grazing; (B) mesozooplankton grazing impact on the standing stock of euphotic zone chl a

On average, nighttime estimates of grazing along the 110°E transect were 65% higher than daytime consumption rates at the same station (Fig. 8A). However, when the grazing estimates were normalized to zooplankton C biomass, the resulting day and nighttime rates were not significantly different (t_{18} = 2.02, p = 0.87) (Fig. 8B). These results do not preclude the possibility that a significant diel cycle in grazing activity might have been found had we sampled more uniformly over the full 24 h day. Nonetheless, a weak or absent diel cycle is more likely given that our early evening (dark) sampling, which showed no C-specific rate increase, should reasonably have captured the peak feeding period of animals, including diel migrants that reduce daytime feeding to minimize predation risk (e.g. Bollens & Sterns 1992). For continuing analyses below, we combined the 12 h daytime and nighttime grazing estimates into full-day biomass-specific rates.

3.4. Temperature relationships and C-based ingestion estimates

C-specific estimates of mesozooplankton grazing showed strong relationships with environmental temperature (Fig. 9). Chl *a* consumption varied by a

factor of 6.6 (1.3 to 8.4 mg chl $a \text{ mgC}^{-1} \text{ d}^{-1}$) over the 11.6-26.5°C temperature range and can be described by the exponential function: mg chl a mgC⁻¹ $d^{-1} = 0.272e^{0.121T^{\circ}C}$, $R^2 = 0.85$ (Fig. 9A). Stn 2 (38°S) was excluded from the data for this relationship because the zooplankton community there was dominated by a high density of pteropod trochophore larvae (Cavolinidae family) with unusually high GPC relative to the copepod-dominated community at adjacent stations and elsewhere on the transect. It is, however, an interesting example of rate sensitivity to compositional variations in the zooplankton community. C-specific clearance rate estimates for the zooplankton community varied by a factor of 13.6, from 5 to $69 \, l \, mgC^{-1} \, d^{-1}$, and can be described by the relationship: $1 \text{ mgC}^{-1} \text{ d}^{-1} = 1.39 e^{0.137 T^{\circ} \text{C}}, R^2 = 0.64$ (Fig. 9B). In terms of the range of rates measured and correlation coefficients, the relationships between DW-specific grazing and temperature (not shown) were very similar to those for C-specific grazing rates (mg chl a mgDW⁻¹ d⁻¹ = $0.078e^{0.127T^{\circ}C}$, R² = 0.87; $1 \text{ mgDW}^{-1} \text{ d}^{-1} = 0.408 \,\mathrm{e}^{0.141 \,\mathrm{T}^{\circ}\mathrm{C}}$, $\mathrm{R}^2 = 0.64$). These relationships indicate that mesozooplankton grazing activity was strongly associated with increasing temperature along the transect, independent of variability in euphotic zone chl a and zooplankton biomass. All relationships between grazing rates and temper-

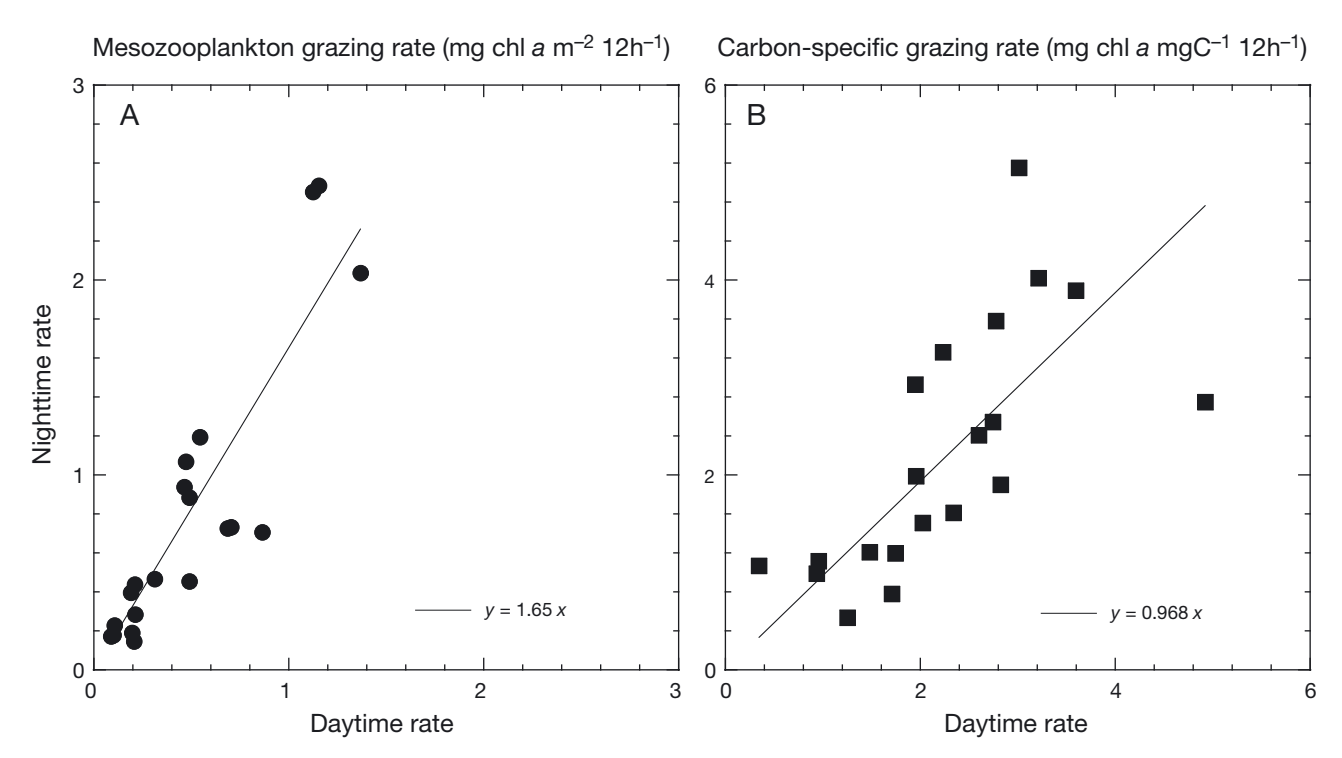


Fig. 8. Relationships between day and night estimates of grazing and carbon-specific grazing rates for mesozooplankton along the 110°E transect. Linear relationships are forced through the origin

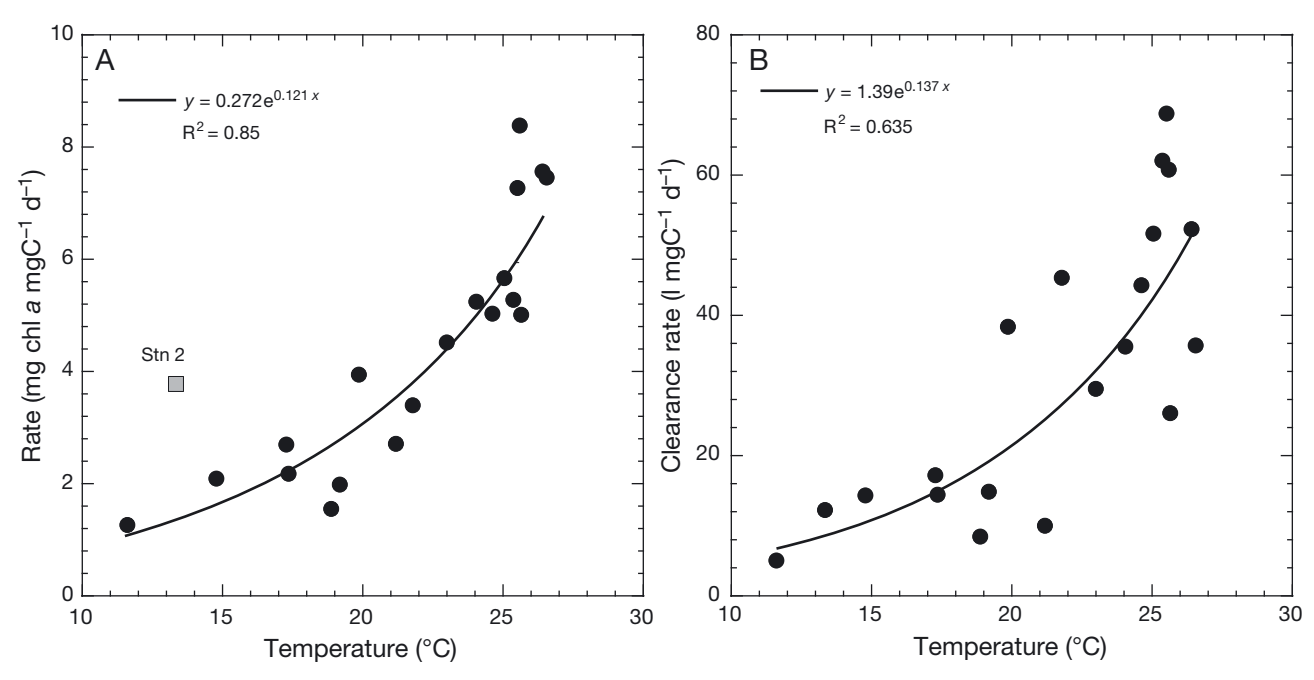


Fig. 9. Relationships between mesozooplankton grazing rate estimates and euphotic zone temperature on the 110°E transect.

(A) Temperature relationship for carbon-specific grazing rate. Data for Stn 2 was anomalous and not included in the regression relationship. (B) Temperature relationship for carbon-specific clearance rate

ature described above were highly significant (p < 0.0001), while there was no significant relationship between C-specific grazing and depth-integrated chl a (chl_{100m}; Table 1) along the transect (r_{18} = 0.30, p > 0.20).

Fig. 10 presents the latitudinal trend in zooplankton ingestion estimates as % of body C consumed daily computed from the C-specific grazing rates on chl a and an assumed C:chl a ratio of 58 (Eppley et al. 1992). With the exception of anomalous Stn 2 (38° S), these ingestion estimates for presumptive direct herbivory are on the order of 10 % of body C d⁻¹ south of

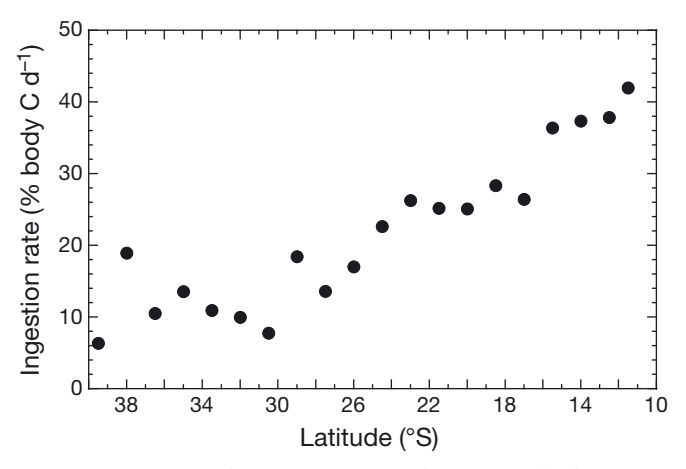


Fig. 10. Estimated ingestion rates of mesozooplankton on the 110° E transect from grazing impact on chl a and an assumed carbon:chl a ratio of 58

 30° S but rise sharply thereafter to ~40% body C d⁻¹ in tropical/ITF water at the northern end of the transect (Fig. 10).

4. DISCUSSION

Two results stand out as the major findings of this study. The first is the substantial increase in zooplankton biomass from subtropical to tropical waters along 110° E. This was expected from historical sampling along the transect and, more generally, from the broadly observed distributions of zooplankton biomass in the oceans, but it provides further documentation and quantification in terms of DW and C measurements. The second major finding is the unexpected increase in biomass-specific grazing along the transect, which we found to be strongly related to environmental temperature and not chl a. In addition, we documented substantial variability in C:DW biomass ratios among stations and size classes, which, while not a new result, clearly complicates comparisons to historical data sets that have not been measured by comparable methods. In the sections below, we first put our biomass findings in the context of previous results for the Indian Ocean and other regions. We then consider the implications of the temperature-dependent grazing relationship for zooplankton energetics and a warming ocean.

4.1. Tropical enrichment of zooplankton biomass

The IN2019_V03 cruise revisited the historical 110°E transect line that was sampled repeatedly by Australian oceanographers from August 1962 to August 1963 as part of the IIOE. On those cruises, depth-integrated vertical tows were done from 200 m to the surface with the Indian Ocean Standard Net (333 µm mesh) and analyzed as wet weight. They are thus difficult to compare directly to our C and DW measurements from shallower oblique tows with a finer mesh net. Nonetheless, the summary of IIOE results by Tranter & Kerr (1969) shows a pattern similar to what we observed, with highest zooplankton biomass north of 14°S, lowest biomass south of 26°S, and relatively uniform values at intermediate latitudes (Figs. 4 & 5). This historical data both informed our expectations before the cruise and puts our measurements in a broader temporal context. Over the IIOE samplings, daytime biomass estimates averaged 59% of nighttime values, similar to our average of 67% (Fig. 4), and transect-averaged biomass during the time of our cruse, the May-June period, was the lowest over the annual cycle. The reported seasonal cycle has 2 peaks, with the major peak in August-September (2-4× the biomass in May-June; Tranter & Kerr 1969), corresponding to the latter stage of the boreal summer SW monsoon (austral winter SE monsoon). The minor peak occurs in February-March during the latter stages of the boreal winter NE monsoon (austral summer NW monsoon). The May-June timing of our cruise coincided with a lower production period in the eastern Indian Ocean, the end of the austral fall intermonsoon. The IIOE historical results indicate that tropical enrichment of zooplankton biomass is a fairly consistent year-long feature of our study region and suggest physical explanations for what may be driving biomass variability on an annual cycle (Tranter & Kerr 1977). Our results confirm that the latitudinal pattern observed 5 decades previously is still evident and quantifiable in terms of measured DW and C biomass. It cannot be explained as an artefact of wet weight measurements of gelatinous zooplankton with high water content.

Indian Ocean samples from IIOE comprise a small but important portion of the database used by Moriarty & O'Brien (2013) in their global synthesis of mesozooplankton biomass distributions. One significant outcome of that analysis is a coarse latitudinal comparison that is consistent with our data in showing approximately 2-fold lower zooplankton C biomass in subtropical to temperate waters of the Southern Hemisphere (15–40°S) compared to lower

latitude (15° N to 15° S) waters. The global analysis, however, shows an increase, rather than a decline in zooplankton biomass for the 15°-40° N zone compared to the tropical region. This difference may reflect the greater concentration of zooplankton biomass measurements around richer coastal margins of the Northern Hemisphere, whereas more of the global data for the tropical sector and the Southern Hemisphere comes from the open ocean. However, in a subsequent analysis of the global biomass distribution of just the macrozooplankton, defined as the larger size (>2 mm) component of the net-caught zooplankton, Moriarty et al. (2013) found dramatically higher biomass in the 15° N- 15° S region (18 ± 26 mg C m⁻³) compared to subtropical latitudes of both the Northern and Southern Hemispheres (0.8 ± 1.3 and 0.3 \pm 0.9 mg C m⁻³, respectively)

Considering only open-ocean expeditions that sampled mesozooplankton biomass across both tropical and subtropical latitudes, there is more of a general pattern of higher zooplankton biomass in tropical waters, particularly at locations that are strongly linked to mechanisms, such as upwelling, that deliver new nutrients to surfaces waters. For example, various crossings of the equatorial Atlantic by the Atlantic Meridional Transect program have shown higher biomass in the equatorial and tropical upwelling regions than in adjacent subtropical waters, although the biomass differences tend to be asymmetrically greater, up to 5-fold, on the southern side compared to a factor of 2 or less on the northern side (Isla et al. 2004, López & Anadón 2008, Calbet et al. 2009). In the central Pacific, sampling along 140° W during the US Joint Global Ocean Flux Study Equatorial Pacific (JGOFS EgPac) program gave a more symmetrical factor-of-2 increase in zooplankton biomass around the equatorial upwelling divergence compared to subtropical waters to the north and south (White et al. 1995), with values similar in magnitude to what we observe in the eastern Indian Ocean. In contrast, in the western Pacific along 160°E, where a thick layer of oligotrophic water in the Western Warm Pool prevents significant nutrient flux into surface waters, the equatorial region is a local minimum in zooplankton biomass (Sun & Wang 2017). We can take from the above examples that tropical enhancement of zooplankton biomass in the eastern Indian Ocean probably requires a mechanism of new nutrient delivery similar in magnitude to that in the equatorial Pacific upwelling region.

Due to EEZ (exclusive economic zone) restrictions, we were not able to sample as far north as the original IIOE cruises, and therefore missed the feature that Tranter & Kerr (1977) determined was responsible for the tropical enrichment of zooplankton biomass, which they called the Java Dome. As originally described by Wyrtki (1962), the formation of the westward-flowing South Equatorial Current south of Java involves an anticyclonic turn of surface currents from the south forming a thermocline dome that strengthens during the SE monsoon. The Costa Rica Dome, a region of elevated productivity zooplankton biomass at ~9°N in the eastern Pacific (Landry et al. 2016), is an analogous seasonally developing feature where enrichment occurs by upwelling on the eddy flank and by lateral transport of deeper water over the thermocline ridge (Wyrtki 1964). Wyrtki (1962) documented that phosphate was substantially elevated at 100 m in the Java Dome region, and Rochford (1977) further described the doming and mixing of nutrient-enriched deep tropical waters to 40-50 m in the euphotic layer north of the South Equatorial Current during the austral winter-spring (May-October) period, though not clearly penetrating into the surface mixed layer. Based on this, Tranter & Kerr (1977) indicated that the area contrasted with classical upwelling systems in not showing a major increase in near-surface nutrients, which suggests that a good deal of the productivity may occur in the lower euphotic zone, as has been observed for massive sub-surface diatom blooms in lee eddies of the Hawaiian Islands (e.g. Brown et al. 2008, Landry et al. 2008). Nonetheless, modern satellite images do show at least some dynamical response in surface ocean color south of Java during winter-spring as well as enrichment off of NW Australia that Tranter & Kerr (1977) linked to the separate feeding aggregation areas for humpback and sperm whales from historical whaling records. Thus, there is ample evidence of enhanced productivity areas that could generate and sustain the elevated zooplankton biomass that we found in tropical waters, even though they were not directly observed in our transect sampling.

In the first depth-resolved analysis of ITF nutrient transport based on volume transport and concentrations, Ayers et al. (2014) revealed surprisingly high NO_3^- -based new production potential. Mixing along the ITF passages is effective in bringing North Pacific thermocline waters upward, such that NO_3^- concentrations average ~5 μM at the surface and 20 μM at 150 m depth in all of the major ITF passages. Almost all of the effective nutrient exchange through the ITF occurs in waters shallower than 400 m, and <150 m in the Lombok Strait, which accounts for ~25 % of ITF volume transport and is the closest outlet to our transport

sect line (115.7°E). Ayers et al. (2014) determined that if all of the ITF NO_3^- delivered to the eastern Indian Ocean was biologically available, the new production f-ratio would be raised by 0.15, on average, over an area 5–6 times that of the Mediterranean Sea. While it is unrealistic to expect this potential to be fully realized, it does suggest a substantial source of NO_3^- to support localized areas of new production from upwelling, advective transport or mesoscale (eddy pumping) mechanisms (Rossi et al. 2013, Dufois et al. 2014).

It may also be that N2 fixation contributes significantly to regional new production. For example, Waite et al. (2013) measured N₂ fixation rates accounting for up to 80% of new production in oligotrophic waters off the west coast of Australia, and Raes et al. (2014) found that Trichodesmium blooms contributed up to 50% of new production along the NW margin of Australia and Timor Sea. For the present 110°E transect study, <2 mm zooplankton size fractions were found to have consistently higher $\delta^{15}N$ values (10.4-10.6 %; Stns 3-5), indicative of nitrate upwelling, near the subtropical front and consistently lower δ^{15} N values (4.2–5.4 ‰; Stns 8–13), suggestive of increasing N2 fixation, in the mixing area (Stns 8-13) between the subtropical and tropical surface water masses (E. J. Raes et al. unpubl. data). Mesozooplankton δ^{15} N values increased in the northern end of the transect (6.0-7.3%; Stns 18-20; E. J. Raes et al. unpubl. data). While much more needs to be done in future studies to understand the relative contributions of nutrient sources that stimulate productivity and zooplankton biomass in tropical waters of the eastern Indian Ocean, the zooplankton enrichment pattern appears more consistent with an increasing role of upward nitrate mixing, rather than N_2 fixation, in the direction of the ITF.

4.2. Temperature-enhanced grazing

Mesozooplankton herbivory, the direct feeding of mesozooplankton on phytoplankton, is classically observed to increase in association with environmental conditions, such as temperate and high-latitude blooms, that stimulate phytoplankton biomass overall, and larger phytoplankton taxa in particular. While it would not have been unexpected to find increased grazing along the 110°E transect in local areas of higher chl *a* and reduced temperature similar to tropical upwelling zones in the Atlantic and Pacific Oceans (Zhang et al. 1995, Isla et al. 2004, López & Anadón 2008, Calbet et al. 2009), the com-

bination of apparent severe oligotrophy and monotonically increasing temperature throughout the subtropical and tropical regions of 110°E comprise unusual, if not unique, circumstances. Mixed-layer concentrations of chl a, in fact, declined somewhat, though not significantly, along with south-to-north increasing temperature over the 110°E transect (Table 1). Such conditions resemble, at least superficially, the predicted effects of climate warming, which anticipate expanding oligotrophic systems that are increasingly unfavorable for mesozooplankton (Richardson 2008, Chust et al. 2014, Stock et al. 2014, Steinberg & Landry 2017). Despite these conditions, however, our results indicate remarkably strong increases in total and biomass-specific grazing along the transect (Figs. 7–9). In addition, while the observed biomass accumulation at northern stations might be connected by transport to a distant high-production area, the much shorter time scale of gut turnover requires that grazing rates be more directly linked to instantaneous measurements of ecosystem properties.

Some of the transect variability in grazing rate estimates can be ascribed to specific factors considered in our analysis. For example, the measured increase in zooplankton biomass along the transect accounts for about a 2-fold range of rate variability, as determined from the ratio of the 14× increase in community grazing on chl a (Fig. 7) compared to the $6.5\times$ increase in biomass-specific grazing on chl a (Fig. 9a). The 13.6× range in biomass-specific clearance rates (Fig. 9) accounts for both transect variability in zooplankton biomass and chl a content of the euphotic zone. Of that, the temperature-dependent gut clearance rate constant for computing grazing rate estimates (Irigoien 1998) accounts for a factor of 2. This leaves approximately a 7-fold temperature enhancement in C-specific chl a clearance rates along the transect that is above and beyond what can explained by variability in zooplankton biomass, chl a concentration and the gut clearance rate function.

Tranter (1977b) distinguished different copepod species groups associated with tropical and subtropical water masses along 110°E. We thus assumed that measured biomass and temperature rate relationships reflected those of different assemblages that are adapted to the range in thermal and trophic conditions along the transect, rather than temperature responses of identical assemblages. We also observed increases in the occurrence of small salps as well as the measured grazing contributions of larger zooplankton at the northern stations (Fig. 7), suggesting a slight shift to larger, more-efficient

grazers of small phytoplankton in the tropical water mass. Overall, however, grazing remained strongly dominated by <2 mm size classes at all of the stations (Fig. 7). Thus, while community composition might contribute to grazing rate variability in subtle ways, it does not explain the general trend relating to temperature.

Whether the increasing trend in mesozooplankton C-based grazing estimates across the 110°E transect (Fig. 10) represents a net positive, negative or neutral contribution to zooplankton C budgets depends on how it compares to the expected effects of temperature on zooplankton energetics and growth requirements. To make those comparisons, we computed respiratory (*R*) requirements from the empirical equation of Ikeda (1985):

$$\ln R_o \ (\mu l \ O_2 \ ind.^{-1} \ h^{-1}) = 0.8354 \times \ln C_i \ (mg \ C \ ind.^{-1}) + 0.0601 \times T \ (^{\circ}C) + 0.5254$$
 (2)

where C_i is the average C content of an individual zooplankter in size-fraction i. Potential growth rates (g, d^{-1}) were similarly computed from the equation of Hirst & Sheader (1997):

$$\log_{10} g (d^{-1}) = -0.2962 \times \log_{10} C_i (\mu g C \text{ ind.}^{-1}) + 0.0246 \times T (^{\circ}C) - 1.1355$$
 (3)

This particular model was used because its predictions agree closely with the zooplankton growth rates supported by food-web flows in the equatorial Pacific (Landry et al. 2020) and, thus, represent the expected growth rates that could be achieved if all nutritional resources, in addition chl a-containing food, were considered. For both respiration and growth rate equations, we used mean estimates of individual zooplankton C (2.4, 7.4, 41, 140 and 2782 μq C ind.⁻¹ for the 0.2–0.5 to >5 mm size fractions, respectively) determined from measured size-fractioned abundances and C biomass in 144 net tows from the subtropical Pacific (Landry et al. 2001). Growth rates (d⁻¹) were converted to production estimates by multiplying by the mean day-night C biomass of the zooplankton assemblage (mg C m⁻²) at each station. Respiration rates for each size class were converted to C equivalents using the molar volume of an ideal gas at standard temperature and pressure (22.4 l mol⁻¹), the respiratory quotient (0.97; Hernández-León & Ikeda 2005) and the molecular weight of C (12 g C mol⁻¹) and multiplying by zooplankton abundance (total C biomass ind.-1). The feeding rates (C demand) needed to satisfy respiration and growth requirements further assume a 70 % absorption efficiency for ingested food (Steinberg & Landry 2017).

Table 2 summarizes transect calculations of Cbased respiration and growth rates (mg C m⁻² d⁻¹) of the zooplankton community as well as the percentage of mesozooplankton C that must be ingested daily to satisfy energetic requirements for respiration only or for the combination of respiration and production. Estimates of community respiration increase by about a factor of 7.7 (12.9 to 99.9 mg C m^{-2} d^{-1}) from the lowest values at Stn 2 to the highest values at Stn 18, and production predictions vary by a factor of 6 (10.2 to 60.9 mg C $m^{-2} d^{-1}$) over the same interval (Table 2). These ranges include the effects of a $3.6\times$ increase in total C biomass, a 13.3°C increase in mean environmental temperature and some variability in size-class contributions to biomass. On a biomass-specific basis, the feeding required to achieve these rates approximately doubles over the temperature range from 13.9 to 29% of zooplankton body C d⁻¹ for respiration only, and from 24 to 48% of body C d⁻¹ for respiration and production together.

C-based estimates of zooplankton ingestion (Fig. 10) fall far short of satisfying the zooplankton energetic requirements in the southern portion of the 110°E

Table 2. Predicted respiration, production and required feeding rates of mesozoo-plankton along the 110°E transect. T: mean recorded temperature over the depth of the net tows. Biomass: average measured total C of day and nighttime net tows at each station. Respiration estimates: based on the empirical metabolic equations of Ikeda (1985), which consider environmental temperature and mean biomass of individuals within zooplankton size classes. Production estimates: based on the empirical growth rate equations of Hirst & Sheader (1997) computed from environmental temperature and mean biomass of individuals within zooplankton size classes. Estimates of required mesozooplankton feeding to satisfy energetic demands of respiration or respiration + production assume a 70% digestive absorption efficiency

	Lat.	$T_{ m mean}$	Biomass	Rate est. (mg C m ⁻² d ⁻¹)		Feeding req. (%C d ⁻¹)		
Stn	(°S)	(°C)	$(mg C m^{-2})$	Resp	Prod		Resp+Prod	
1	39.5	11.6	264	24.4	20.3	13.2	24.2	
2	38.0	13.3	132	12.9	10.2	13.9	24.9	
3	36.5	14.8	133	14.5	11.6	15.6	28.0	
4	35.0	17.3	131	16.9	13.6	18.5	33.3	
5	33.5	17.4	297	35.2	26.2	16.9	29.5	
6	32.0	19.2	131	16.4	11.4	17.8	30.3	
7	30.5	18.9	249	34.0	26.3	19.5	34.6	
8	29.0	19.9	159	22.5	17.0	20.2	35.4	
9	27.5	21.2	286	39.3	26.9	19.6	33.1	
10	26.0	21.8	278	41.5	29.7	21.3	36.6	
11	24.5	23.0	318	51.1	35.6	23.0	39.0	
12	23.0	24.0	293	51.4	36.8	25.0	42.9	
13	21.5	24.6	279	49.7	35.2	25.5	43.5	
14	20.0	25.6	274	51.8	36.2	27.0	45.1	
15	18.5	25.1	307	56.7	40.1	26.4	45.0	
16	17.0	25.4	268	48.9	33.2	26.1	43.8	
17	15.5	25.5	216	42.3	31.0	28.0	48.5	
18	14.0	26.6	488	99.9	71.9	29.3	50.3	
19	12.5	26.4	450	92.6	67.0	29.4	50.7	
20	11.5	25.6	426	84.2	60.9	28.2	48.6	

transect (Stns 1-10, south of 26°S), where water temperature was coldest and chl a highest. Considering only the component of feeding measured by gut pigment (i.e. not accounting for food resources lacking chl a), the average feeding rate deficiency in this region was -3% of body C d⁻¹ for respiration and -16% d⁻¹ for the combined requirements for respiration and production. A different picture emerges for the northern half of the transect (Stns 11-20), where accelerating ingestion gradually satisfies respiration (+9% of body C d-1, on average) and reduces the feeding deficiency for combined respiration and production (-10% of body C d⁻¹, on average). According to these estimates, ingestion comes closest to balancing energetic requirements $(-5.0\% \text{ of body C d}^{-1}; \text{ Stns } 17-20) \text{ in tropical waters}$ with the highest temperature. Our conclusion from this comparison is that the C-based ingestion rates estimated from gut pigments on the 110°E transect increased faster with increasing temperature than the predicted effect of temperature on C demand for respiration and growth. As a consequence, the temperature-enhanced grazing trend makes a net

positive contribution to the energy balance of zooplankton.

The above estimates for feeding rate contributions to energetic requirements are similar in magnitude to those reported by López & Anádon (2008) for the equatorial Atlantic but substantially higher than commonly found for oligotrophic oceans. López & Anádon (2008) gave biomass-specific grazing estimates as high as 80-90 % of body $C\ d^{-1}$ for some zooplankton size fractions, and their mean rates computed from measured total biomass and grazing and an assumed C:chl a = 58, exactly as we have done here, gave C-specific ingestion rates of 43% (upwelling), 24% (equatorial), 12% (N subtropics) and 16% (S subtropics) of body C d⁻¹ for the various regions studied. In contrast, most studies in the lowlatitude oceans have shown that herbivory fails to meet even the C demand for respiration (Zhang et al. 1995, Roman et al. 2002, Calbet et al. 2009), leading to the widely held, and experimentally supported, view that most zooplankton

nutrition in the open ocean is provided by predation on microzooplankton (Calbet 2001, Calbet & Saiz 2005, Landry & Décima 2017) or from general omnivorous feeding on varying food resources, including detritus.

Our high estimates of zooplankton herbivory do not necessarily represent a departure from the expected importance of microzooplankton as the primary grazers and trophic intermediaries to mesozooplankton in the open ocean (Calbet & Landry 2004), but do highlight a significant uncertainty in applying gut clearance rate constants to the grazing calculations. We chose the Irigoien (1998) relationship because it was based on a large body of experimental data and had a relatively conservative temperature function (Fig. 2). However, the data for high temperatures are sparse, and the extrapolation of largely temperate results to tropical temperatures introduces a large multiplier into the rate determinations. For comparison, López & Anádon (2008) measured gut clearance rates between 14 and 21°C along their Atlantic transect that are about 60% of the values that we used at comparable temperatures. Several experiments done at >28°C in the South China Sea have also given mean rates $(0.027 \text{ min}^{-1}; \text{Tseng et al.})$ 2009) that are one-third the value of what the Irigoien (1998) relationship would predict. If our rates are scaled by either of these lower factors, the 110°E zooplankton assemblages would require very much higher contributions from microzooplankton predation or general omnivory to meet energetic and growth requirements. Nonetheless, the conclusions of (1) a temperature-enhanced grazing trend and (2) a positive energetic contribution of the trend are robust. This is because even if a constant estimate of gut clearance rate is applied to all grazing calculations regardless of temperature, the remaining 7-fold increase in C-specific *GPCs* greatly exceeds the predicted 2.5 and 2.3× increases in biomass-specific respiration and growth rates, respectively, over the temperature range of the transect.

4.3. Implications for a warming ocean

Although the Indian Ocean is the smallest and least studied of the major oceans, it has many unique features of geography and circulation that amplify its role in global climate dynamics (Hermes et al. 2019). One of those features, the ITF, is the only low-latitude connection between oceans, through which water and heat transfer from the Pacific has made the Indian Ocean the fastest warming ocean over the

past 2 decades (Lee et al. 2015, Desbruyères et al. 2017). Recent analyses suggest that the development of previously unknown transport pathways of ITF into the interior of Indian Ocean have lengthened the passage (residence) time of waters that ultimately exit to the Atlantic, with associated effects on temperature, stratification and rainfall (Makarim et al. 2019). Gregg & Rousseaux (2019) further pointed to the equatorial and north Indian Ocean as being responsible for most of the global decline in satelliteestimated ocean productivity over the same period. Despite its small size, the ITF region between Indonesia and NW Australia is also a hotspot of biodiversity (e.g. Sutton & Beckley 2017) and fisheries, including the only global spawning area for southern bluefin tuna (Matsuura et al. 1997, Farley et al. 2015). It is, therefore, a region where improved understanding of ecological relationships is desirable in its own

As for any region, the accuracy of future climate predictions for the eastern Indian Ocean requires a good understanding of the mechanisms that drive patterns and dynamics in the contemporary ocean. By this metric, ocean ecosystem models have shown mixed degrees of skill for our study region. According to the C-based satellite estimates of Behrenfeld et al. (2005), phytoplankton growth rates and productivity are high in the ITF region, comparable to rates in equatorial areas of the Atlantic and Pacific Oceans. Compared to the same equatorial regions, however, trophic models based on satellite productivity suggest much lower values of zooplankton biomass and phytoplankton:zooplankton biomass ratios in our study area (e.g. Strömberg et al. 2009, Ward et al. 2012). Part of this discrepancy might be explained by differences in how ecosystem models structure trophic interactions (Sailley et al. 2013) or by uncertainties, in particular, in the temperature sensitivities of tropical production systems (Kwiatkowski et al. 2017). However, many models have emphasized the significance of elevated temperature in amplifying the propagation of phytoplankton biomass trends to higher trophic levels at low latitudes, which make the projected impacts of future temperature increases on zooplankton substantially higher than the impacts on phytoplankton (Chust et al. 2014, Stock et al. 2014, Kwiatkowski et al. 2019). Stock et al. (2014) ascribed this trophic amplification to 3 temperature effects—decreasing fraction of primary production consumed due to smaller phytoplankton, increasing zooplankton trophic positions due to a dietary shift to microzooplankton or carnivory and decreasing growth efficiencies due to higher metabolic costs.

While we do not dispute experimental and observational findings that underly the concept of trophic amplification, our biomass and grazing results suggest that the coupling between primary producers and mesozooplankton in tropical systems could be more efficient than conventionally assumed. Similar to our findings, López & Anadón (2008) observed their highest grazing impact on phytoplankton productivity in the equatorial Atlantic. Copepods from that region also had larger mean size than those in adjacent subtropical waters with similar phytoplankton size structure and equal or higher rates of biomass-specific grazing than in temperate waters with large phytoplankton. López & Anadón (2008) attributed these findings to zooplankton assemblages acclimated or adapted to feed more efficiently on small cells. More recently, Boersma et al. (2016) advanced an energetic argument for why increased zooplankton herbivory might be expected as the oceans warm, suggesting that the higher C content of primary producers is more desirable for satisfying the higher metabolic C demand at higher temperature, with isotopic analyses and laboratory feeding studies providing some support for this hypothesis. While interpretation of this evidence is not without controversy (Winder et al. 2016), we note here that the strong relationship between zooplankton herbivory and temperature on the 110°E transect are fieldbased results consistent with the Boersma et al. (2016) prediction.

Another possible mechanism for improving food web efficiency and higher apparent zooplankton grazing on phytoplankton in tropical waters would be a temperature shift toward greater mixotrophy, referring to the collective diverse strategies by which pelagic protists assume the functions of both primary producer and micro-consumer (Stoecker 1998). Because mixotrophs produce C as needed by photosynthesis to fuel metabolism, their grazing-acquired nutrients are better retained and applied efficiently to growth (Raven 1997, Rothhaupt 1997, Mitra et al. 2014). The combined photosynthetic and phagotrophic functions of mixotrophs also shorten mean food chain length, thereby enhancing the efficiency of trophic transfer to mesozooplankton (Mitra et al. 2014, Ward & Follows 2016). Although mixotrophy is known to be important, particularly in high-light, low-nutrient systems, there are too few direct rate measurements to compare ecosystems, latitudinal zones or temperatures. Data biases are also evident with respect to cell sizes, taxa and regions studied, with most observations focused on large dinoflagellates in coastal and high-latitude environments

(Leles et al. 2019). We suggest that higher temperature could be a factor in selecting for increased mixotrophy in low-nutrient tropical seas to achieve faster and more efficient growth driven by high grazing pressure and biomass turnover. The strong relationship between zooplankton grazing and temperature in the present study is consistent with this hypothesis, with the caveat that our grazing estimates on chl a-containing cells would also include all or most of the food intake traditionally assumed to come separately via predation on microzooplankton. That would put the high C-specific ingestion rates in Fig. 10 in a different perspective, as more indicative of total transfer though the microbial food web rather than an estimate for just phytoplankton.

Lastly, while we have viewed the consistently low mixed-layer nutrients and chl a over most of the 110°E transect as an indication of a comparable degree of oligotrophy, they could instead be a manifestation of top-down grazer control. Mesocosm experiments indicate that warming alters food web structure by strengthening grazer control of primary production, especially as the rate of nutrient supply increases (O'Connor et al. 2009), as might well be the case for ITF-influenced tropical water mass. Thus, the combination of warmer temperature and higher nutrient fluxes (not necessarily higher mixed-layer concentrations) in the tropical waters may drive higher grazing that suppresses chl a. Ocean ecosystem models consistent with this mechanism have further suggested that the ITF region may be one of the few low-latitude systems where nutrient fluxes increase with temperature by 2100 (Lewandowska et al. 2014).

The original IIOE-110°E investigators could scarcely have imagined an ocean in which bacteria had major food web roles, protists were the dominant consumers of primary production, phytoplankton were likely grazers and rapidly rising temperature was a matter of global concern. In another half century, our current understanding of ocean processes and ability to model and predict climate change consequences may seem equally naive. One potential message to take away from the unexpected finding of a positive temperature response in zooplankton C-specific grazing across an apparently nutrient-poor region of the subtropical-tropical ocean is that our present understanding of the effects of warming may not be as settled as they appear in simple trophic models and thinking derived mainly from studies of temperate and high-latitude ecosystems. Like the Indian Ocean generally, tropical regions of the

oceans directly effect a disproportionate fraction of the global population and will likely bear much of the negative impact of climate warming, yet they are understudied in almost every respect. Future studies are needed that examine in detail the food web structure, nutrient fluxes and trophic dynamics of tropical ocean regions and their temperature sensitivities.

Acknowledgements. We gratefully acknowledge the exceptional leadership of Chief Scientist, Lynnath Beckley, and the professionalism and good spirits of the captain, crew and shipmates of the R/V 'Investigator', who supported and facilitated the shipboard research in innumerable ways. We specifically thank the CSIRO hydrography/hydrochemistry team and technical support group for CTD and nutrient data that appear in Fig. 3 and Table 1. Kelsey Fleming, Tabitha Hernandez and Bruce Deck assisted with laboratory analyses. Data analyses were supported in part by National Science Foundation Grant OCE-1851558 to M.R.L. Zooplankton net tows at Stns 8-12 (29°-23°S, 110°E) were taken under Australian Fisheries Management Authority scientific permit 1004152, Australian Government permit AU-COM2019-446 and those in the Abrolhos Marine Park under permit PA2018-00065-1 issued by the Director of National Parks, Australia. The views expressed in this publication do not necessarily represent those of the Director of National Parks, CSIRO or the Australian Government.

LITERATURE CITED

- Ayers JM, Strutton PG, Coles VJ, Hood RR, Matear RJ (2014) Indonesian throughflow nutrient fluxes and their potential impact on Indian Ocean productivity. Geophys Res Lett 41:5060–5067
- Behrenfeld MJ, Boss E, Siegel DA, Shea DM (2005) Carbonbased ocean productivity and phytoplankton physiology from space. Global Biogeochem Cycles 19:GB1006
- Boersma M, Mathew KA, Niehoff B, Schoo KL, Franco-Santos RM, Meunier CL (2016) Temperature driven changes in the diet preference of omnivorous copepods: No more meat when it's hot? Ecol Lett 19:45–53
- Bollens SM, Sterns DE (1992) Predator-induced changes in the diel feeding cycle of a planktonic copepod. J Exp Mar Biol Ecol 156:179–186
- Brown SL, Landry MR, Selph KE, Yang EJ, Rii YM, Bidigare RR (2008) Diatoms in the desert: phytoplankton community response to a mesoscale eddy in the subtropical North Pacific. Deep Sea Res II 55:1321–1333
- Calbet A (2001) Mesozooplankton grazing effect on primary production: a global comparative analysis in marine ecosystems. Limnol Oceanogr 46:1824–1830
- Calbet A, Landry MR (2004) Phytoplankton growth, microzooplankton grazing, and carbon cycling in marine systems. Limnol Oceanogr 49:51–57
- Calbet A, Atienza D, Henriksen CI, Saiz E, Adey TR (2009) Zooplankton grazing in the Atlantic Ocean: a latitudinal study. Deep Sea Res II 56:954–963

- Chust G, Allen JI, Bopp L, Schrum C and others (2014) Biomass changes and trophic amplification of plankton in a warmer ocean. Glob Change Biol 20:2124–2139
- Conover RJ, Durvasula R, Roy S, Wang R (1986) Probable loss of chlorophyll-derived pigments during passage through the gut of zooplankton, and some of the consequences. Limnol Oceanogr 31:878–887
- Dam HG, Peterson WT (1988) The effect of temperature on the gut clearance rate constant of planktonic copepods. J Exp Mar Biol Ecol 123:1–14
- Desbruyères D, McDonagh EL, King BA, Thierry V (2017) Global and full-depth ocean temperature trends during the early 21st century from Argo and repeat hydrography. J Clim 30:1985–1997
- Dufois F, Hardman-Mountford NJ, Greenwood J, Richardson AJ, Feng M, Herbette S, Matear R (2014) Impact of eddies on surface chlorophyll in the South Indian Ocean. J Geophys Res Oceans 119:8061–8077
- Durbin EG, Campbell RG (2007) Reassessment of the gut pigment method for estimating *in situ* zooplankton ingestion. Mar Ecol Prog Ser 331:305–307
- Eppley RW, Chavez FP, Barber RT (1992) Standing stock of particulate carbon and nitrogen in the equatorial Pacific at 150° W. J Geophys Res 97:655–661
- Farley JH, Davis TLO, Bravington MV, Andamari R, Davies CR (2015) Spawning dynamics and size related trends in reproductive parameters of southern bluefin tuna, *Thunnus maccoyii*. PLOS ONE 10:e0125744
- Gregg WW, Rousseaux CS (2019) Global ocean primary production trends in the modern ocean color satellite record (1998–2015). Environ Res Lett 14:124011
- Hermes JC, Masumoto Y, Beal LM, Roxy MK and others (2019) A sustained ocean observing system in the Indian Ocean for climate related scientific knowledge and societal needs. Front Mar Sci 6:355
- Hernández-León S, Ikeda T (2005) A global assessment of mesozooplankton respiration in the ocean. J Plankton Res 27:153–158
- Hirst AG, Sheader M (1997) Are in situ weight-specific growth rates body-size independent in marine planktonic copepods? A re-analysis of the global synthesis and a new empirical model. Mar Ecol Prog Ser 154:155–165
- Humphrey GF, Kerr JD (1969) Seasonal variation in the Indian Ocean along 110° E. III. Chlorophylls *a* and *c*. Aust J Mar Freshwater Res 20:55–64
- *Ikeda T (1985) Metabolic rates of epipelagic marine zooplankton as a function of body size and temperature. Mar Biol 85:1-11
- ĭIsla JA, Llope M, Anadón R (2004) Size-fractionated mesozooplankton biomass, metabolism and grazing along a 50°N−30°S transect of the Atlantic Ocean. J Plankton Res 26:1301−1313
- Jitts HR (1969) Seasonal variation in the Indian Ocean along 110°E. IV. Primary production. Aust J Mar Freshwater Res 20:65–75
- Kleppel GS, Pieper RE (1984) Phytoplankton pigments in the gut contents of planktonic copepods from coastal waters off Southern California. Mar Biol 78:193–198
- Kwiatkowski L, Bopp L, Aumont O, Ciais P and others (2017) Emergent constraints on projections of declining primary production in the tropical oceans. Nat Clim Chang 7: 355–359

- Kwiatkowski L, Aumont O, Bopp L (2019) Consistent trophic amplification of marine biomass declines under climate change. Glob Change Biol 25:218–229
- Landry MR, Décima MR (2017) Protistan microzooplankton and the trophic position of tuna: quantifying the trophic link between micro- and mesozooplankton in marine foodwebs. ICES J Mar Sci 74:1885–1892
- Landry MR, Lorenzen CJ, Peterson WK (1994) Mesozooplankton grazing in the Southern California Bight. 2. Grazing impact and particulate flux. Mar Ecol Prog Ser 115:73–85
- Landry MR, Al-Mutairi H, Selph KE, Christensen S, Nunnery S (2001) Seasonal patterns of mesozooplankton abundance and biomass at Station ALOHA. Deep Sea Res II 48:2037–2061
- *Landry MR, Brown SL, Rii YM, Selph KE, Bidigare RR, Yang EJ, Simmons MP (2008) Depth-stratified phytoplankton dynamics in Cyclone Opal, a subtropical mesoscale eddy. Deep Sea Res II 55:1348–1359
- Landry MR, De Verneil A, Goes JI, Moffett JW (2016) Plankton dynamics and biogeochemical fluxes in the Costa Rica Dome: introduction to the CRD Flux and Zinc Experiments. J Plankton Res 38:167–182
- *Landry MR, Stukel MR, Décima MR (2020) Food-web fluxes support high rates of mesozooplankton respiration and production in the equatorial Pacific. Mar Ecol Prog Ser (in press), doi:10.3354/meps13479
- Lavaniegos BE, Ohman MD (2003) Long-term changes in pelagic tunicates of the California Current. Deep Sea Res II 50:2473–2498
- Lee SK, Park W, Baringer MO, Gordon A, Huber B, Liu Y (2015) Pacific origin of the abrupt increase in Indian Ocean heat content during the warming hiatus. Nat Geosci 8:445–450
- Leles SG, Mitra A, Flynn KJ, Tillmann U and others (2019) Sampling bias misrepresents the biogeographical significance of constitutive mixotrophs across global oceans. Glob Ecol Biogeogr 28:418–428
- Lewandowska AM, Boyce DG, Hofmann M, Matthiessen B, Sommer U, Worm B (2014) Effects of sea surface warming on marine plankton. Ecol Lett 17:614–623
- López E, Anadón R (2008) Copepod communities along an Atlantic Meridional Transect: abundance, size structure and grazing rates. Deep Sea Res I 55:1375–1391
- Makarim S, Sprintall J, Liu Z, Yu W, Santoso A, Yan XH, Susanto RD (2019) Previously unidentified Indonesian Throughflow pathways and freshening in the Indian Ocean during recent decades. Sci Rpt 9:7364
- Matsuura H, Sugimoto T, Nakai M, Tsuji S (1997) Oceanographic conditions near the spawning ground of southern bluefin tuna; northeastern Indian Ocean. J Oceanogr 53:421–433
- Mitra A, Flynn KJ, Burkholder JM, Berge T and others (2014) The role of mixotrophs in the biological carbon pump. Biogeosciences 11:995–1005
- Moriarty R, O'Brien TD (2013) Distribution of mesozooplankton biomass in the global ocean. Earth Syst Sci Data 5:45–55
- Moriarty R, Buitenhuis ET, Le Quére C, Gosselin MP (2013)
 Distribution of known macrozooplankton abundance
 and biomass in the global ocean. Earth Syst Sci Data 5:
 241–257
- Newell BS (1969) Seasonal variations in the Indian Ocean along 110°E. II. Particulate carbon. Aust J Mar Freshwater Res 20:51–54

- O'Connor MI, Piehler MF, Leech DM, Anton A, Bruno JF (2009) Warming and resource availability shift food web structure and metabolism. PLOS Biol 7:e1000178
- Raes EJ, Waite AM, McInnes AS, Olsen H, Nguyen HM, Hardman-Mountford N, Thompson PA (2014) Changes in latitude and dominant diazotrophic community alter N₂ fixation. Mar Ecol Prog Ser 516:85–102
- Raven JA (1997) Phagotrophy in phototrophs. Limnol Oceanogr 42:198–205
- Richardson AJ (2008) In hot water: zooplankton and climate change. ICES J Mar Sci 65:279-295
- Rochford DJ (1969) Seasonal variation in the Indian Ocean along 110°E. I. Hydrological structure of the upper 500 m. Aust J Mar Freshwater Res 20:1–50
- Rochford DJ (1977) Further studies of plankton ecosystems in the eastern Indian Ocean. II. Seasonal variations in water mass distribution (upper 150 m) along 110°E. (August 1962–August 1963). Aust J Mar Freshwater Res 28:541–555
- Roemmich D, McGowan JA (1995) Climatic warming and the decline of zooplankton in the California Current. Science 267:1324–1326
- Roman MR, Dam HG, Le Borgne R, Zhang X (2002) Latitudinal comparison of equatorial Pacific zooplankton.

 Deep Sea Res II 49:2695–2711
- Rossi V, Feng M, Pattiaratchi C, Roughan M, Waite AM (2013) On the factors influencing the development of sporadic upwelling in the Leeuwin Current system. J Geophys Res Oceans 118:3608–3621
- Rothhaupt KO (1997) Nutrient turnover by freshwater bacterivorous flagellates: differences between a heterotrophic and mixotrophic chrysophyte. Aquat Microb Ecol 12:65–70
- Sailley SF, Vogt M, Doney SC, Aita MN and others (2013) Comparing food web structures and dynamics across a suite of global marine ecosystem models. Ecol Modell 261-262:43-57
- Steinberg DK, Landry MR (2017) Zooplankton and the ocean carbon cycle. Annu Rev Mar Sci 9:413–444
- Stock CA, Dunne JP, John JG (2014) Drivers of trophic amplification of ocean productivity trends in a changing climate. Biogeosciences 11:7125–7135
- Stoecker DA (1998) Conceptual models of mixotrophy in planktonic protists and some ecological and evolutionary implications. Eur J Protistol 34:281–290
 - Strickland JDH, Parsons TR (1972) A practical handbook of seawater analysis. Fisheries Research Board of Canada, Ottawa
- Strömberg KHP, Smyth TJ, Allen JI, Pitois S, O'Brien TD (2009) Estimation of global zooplankton biomass from satellite ocean colour. J Mar Syst 78:18–27
- Sun D, Wang C (2017) Latitudinal distribution of zooplankton communities in the western Pacific along 160°E during summer 2014. J Mar Syst 169:52–60
- Sutton AL, Beckley LE (2017) Species richness, taxonomic distinctness and environmental influences on euphausiid zoogeography in the Indian Ocean. Diversity (Basel) 9:23
- Taylor AG, Landry MR (2018) Phytoplankton biomass and size structure across trophic gradients in the southern California Current and adjacent ocean ecosystems. Mar Ecol Prog Ser 592:1–17
 - Tomczak M, Godfrey SJ (1994) Regional oceanography: an introduction. Pergamon, Oxford
- Tranter DJ (1977a) Further studies of plankton ecosystems in the eastern Indian Ocean. I. The study and the study area. Aust J Mar Freshwater Res 28:529–539

- Tranter DJ (1977b) Further studies of plankton ecosystems in the eastern Indian Ocean. V. Ecology of the Copepoda. Aust J Mar Freshwater Res 28:593–625
- Tranter DJ, Kerr JD (1969) Seasonal variation in the Indian Ocean along 110°E. V. Zooplankton biomass. Aust J Mar Freshwater Res 20:77–84
- Tranter DJ, Kerr JD (1977) Further studies of plankton ecosystems in the eastern Indian Ocean. III. Numerical abundance and biomass. Aust J Mar Freshwater Res 28: 557–583
- Tseng LC, Dahms HU, Chen QC, Hwang JS (2009) Copepod feeding study in the upper layer of the tropical South China Sea. Helgol Mar Res 63:327–337
- Waite AM, Rossi V, Roughan M, Tilbrook B and others (2013) Formation and maintenance of high-nitrate, low pH layers in the eastern Indian Ocean and the role of nitrogen fixation. Biogeosciences 10:5691–5702
- Ward BA, Follows MJ (2016) Marine mixotrophy increases trophic transfer efficiency, mean organism size, and vertical carbon flux. Proc Natl Acad Sci USA 113: 2958–2963
- Ward BA, Dutkiewicz S, Jahn O, Follows MJ (2012) A sizestructured food-web model for the global ocean. Limnol Oceanogr 57:1877–1891
- White JR, Zhang XS, Welling LA, Roman MR, Dam HG (1995) Latitudinal gradients in zooplankton biomass in

Editorial responsibility: Antonio Bode, A Coruña, Spain

- the tropical Pacific at 140°W during the JGOFS EqPac study: effects of El Niño. Deep Sea Res II 42:715–733
- Wijffels S, Sprintall J, Fieux M, Bray N (2002) The JADE and WOCE I10/IR6 throughflow sections in the southeast Indian Ocean. Part 1: water mass distribution and variability. Deep Sea Res II 49:1341–1362
- Winder M, Burian A, Landry MR, Montagnes DJS, Nielsen JM (2016) Technical comment on Boersma et al. (2016) Temperature driven changes in the diet preference of omnivorous copepods: No more meat when it's hot? Ecology Letters, 19, 45–53. Ecol Lett 19:1389–1391
- Woo M, Pattiaratchi C (2008) Hydrography and water masses off the western Australian coast. Deep Sea Res I 55:1090-1104
- Wyrtki K (1962) The upwelling in the region between Java and Australia during the south-east monsoon. Aust J Mar Freshwater Res 13:217–225
 - Wyrtki K (1964) Upwelling in the Costa Rica dome. Fish Bull 63:355–372
 - Wyrtki K (1973) Physical oceanography of the Indian Ocean. In: Zeitzschel B (ed) Ecological studies: analysis and synthesis, Vol 3. Springer, Berlin, p 18–36
- Zhang X, Dam HG, White JR, Roman MR (1995) Latitudinal variations in mesozooplankton grazing and metabolism in the central tropical Pacific during the US JGOFS EqPac study. Deep Sea Res II 42:695-714

Submitted: February 24, 2020; Accepted: July 23, 2020 Proofs received from author(s): September 3, 2020